9376 *Macromolecules* **2010**, *43*, 9376–9383
DOI: 10.1021/ma101491c

Macromolecules
ARTICLE

Alternating Copolymers of Carbazole and Triphenylamine with Conjugated Side Chain Attaching Acceptor Groups: Synthesis and Photovoltaic Application

Zhi-Guo Zhang,[†] Yi-Liang Liu,[‡] Yang Yang,[†] Keyue Hou,[†] Bo Peng,[†] Guangjin Zhao,[†] Maojie Zhang,[†] Xia Guo,[†] En-Tang Kang,[‡] and Yongfang Li*,[†]

[†]*Beijing National Laboratory for Molecular Sciences, Institute of Chemistry, Chinese Academy of Sciences, Beijing 100190, China, and* [‡]*Department of Chemical & Biomolecular Engineering, National University of Singapore, Kent Ridge, Singapore 119260*

Received July 4, 2010; Revised Manuscript Received October 16, 2010

ABSTRACT: Four alternating copolymers of carbazole (Cz) and triphenylamine (TPA) with thienylene-vinylene (TV) conjugated side chain containing different acceptor end groups of aldehyde (**PCzTPA−TVCHO**), monocyano (**PCzTPA−TVCN**) dicyano (**PCzTPA−TVDCN**), and 1,3-diethyl-2-thiobarbituric acid (**PCzTPA−TVDT**), have been designed and synthesized. The structures and properties of the main chain donor-side chain acceptor D−A copolymers were fully characterized. Through changing the acceptor group attached to the TV conjugated side chain on TPA, the electronic properties and energy levels of the copolymers were effectively tuned. The effect of substituent on the electronic structures of the copolymers was also studied by molecular simulation. These results indicate that it is a simple and effective approach to tune the bandgap in a conjugated polymer by attaching an acceptor end group on the conjugated side chains. **PCzTPA−TVCN**, **PCzTPA−TVDCN**, and **PCzTPA−TVDT** were used as donor in polymer solar cells; the device based on **PCzTPA−TVDT**/$PC_{70}BM$ demonstrates a power conversion efficiency of 2.76% with V_{oc} of 0.87 V under the illumination of AM1.5G, 100 mW/cm^2.

Introduction

Polymer solar cells (PSCs) are considered as a promising alternative to inorganic semiconductor-based solar cells for the generation of affordable, clean, and renewable energy.[1] PSCs are commonly composed of a blend film of conjugated polymer donor and fullerene derivative (such as PCBM) acceptor sandwiched between an ITO positive electrode and a low workfunction metal negative electrode. Advantages of the PSCs include low-cost fabrication of large-area devices, lightweight, mechanical flexibility, and easy tunability of chemical properties of the organic photovoltaic materials. Therefore, there have been great interests from academia to application-oriented companies to increase the efficiency of PSCs for future commercial application, primarily through development of new conjugated polymers[2−4] and device engineering.[5−7] It has been realized that an ideal polymer donor in PSCs should exhibit broad absorption with high absorption coefficient in the visible region, high hole mobility, suitable energy level matching with the fullerene acceptor, and appropriate compatibility with fullerene acceptor to form nanoscale bicontinuous interpenetrating network.[8] Optimization of the properties will offer high values of short-circuit current density (J_{sc}), open-circuit voltage (V_{oc}), and fill-factor (FF) of the PSCs. Power conversion efficiency (PCE) of the PSCs depends on the parameters by the following equation: PCE = $(J_{sc} \times V_{oc} \times FF)/P_{in}$, where P_{in} is the input light power.[9]

One feasible approach toward broadening the visible absorption and tuning the energy levels is to design alternating donor−acceptor (D−A) copolymers, in which the hybridization of HOMO located on the donor moiety with LUMO located on the acceptor moiety provides a means for narrowing the bandgap and tuning the HOMO and LUMO energy levels of conjugated polymers.[10,11] On the basis of this approach, main chain D−A copolymers have been witnessed great success for achieving high performance PSCs.[12−22] However, main chain D−A copolymers may suffer from lower hole mobility due to the influence of the acceptor units on the polymer main chain.

Previous studies in our group have developed a new family of conjugated polymers with conjugated side chains.[2] This type of polymers features high hole mobility thanks to the overlapping of the side chain interactions with the conjugated main chains, and broad absorptions deriving from both the main chains and the conjugated side chains, thus demonstrated prominent device performances in PSCs[23] and OFETs (organic field-effect transistors).[24] Here, we are trying to attach appropriate acceptor end groups to the conjugated side chains to construct new D−A copolymers with main chains as donor unit and side chains as acceptor unit. Compared with well developed main chain D−A copolymers, these main chain donor and side chain acceptor D−A copolymers are expected to have some interesting features for optoelectronic applications, such as higher hole mobility of the polymer main chains and having the advantage of allowing charge separation through sequential transfer of electrons from the main chains to the acceptor side chains and then to fullerene acceptor in the active layer of PSCs.[25] As successful examples, Huang et al recently reported copolymers of fluorene (or silafluorene) and triphenylamine (TPA) with the side chains containing acceptor unit, which exhibited promising photovoltaic properties.[26,27]

Poly(2,7-carbazole) derivatives are among the most promising conjugated polymers used in fabricating the optoelectronic devices.[28,29] They possess the advantages of high hole mobility,

*Corresponding author. E-mail: liyf@iccas.ac.cn.

 Published on Web 10/29/2010

Scheme 1. Synthesis Route of PCzTPA−TVCHO

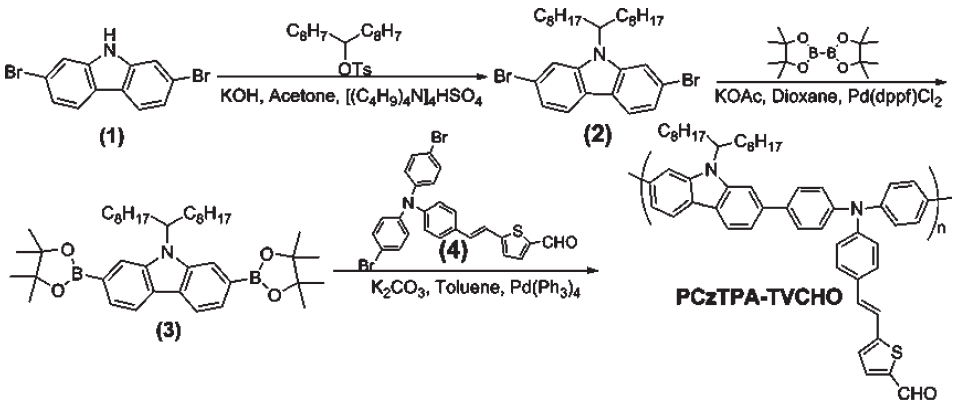

good solution processability, deeper HOMO energy level and air stable features, deriving from the nature of the carbazole unit, such as rigid biphenyl unit, delocalization of the lone electron pair of nitrogen atom over aromatic structure and the bulky alkyl chains attached. The alternating copolymers of 2,7-carbazole and various acceptors have been synthesized for applications as the donor materials in PSCs.[17,29−31] The combination of the unique features of the 2,7-carbazole and the advantages of the main chain donor-side chain acceptor architecture may offers some promising donor materials for high-performance PSCs.

On the basis of the consideration mentioned above, alternating copolymers of 2,7-carbazole and TPA with thienylenevinylene conjugated side chain containing various acceptor end groups including aldehyde (**PCzTPA−TVCHO**), monocyano (**PCzTPA−TVCN**) dicyano (**PCzTPA−TVDCN**), and 1,3-diethyl-2-thiobarbituric acid (**PCzTPA−TVDT**), were designed and synthesized in this work, for the application as donor materials in PSCs. Among the four polymers, **PCzTPA−TVDT** shows broad absorption band in the visible region with absorption edge at 710 nm and promising photovoltaic properties.

Experimental Section

Materials. 9-Heptadecane *p*-toluenesulfonate and 2-[2-[4-[*N*, *N*- di(4-bromophenyl) amino]phenyl]ethenyl]thien-5-al (compound **4** in Scheme 1) were prepared according to the method reported in the literatures.[26,32] Tetrakis(triphenylphosphine)palladium, trioctylmethylammonium chloride (Aliquat 336), octyl cyanoacetate, malononitrile and 1,3-diethyl-2-thiobarbituric acid were purchased from Sigma-Aldrich Chemical Co, while 2,7-dibromocarbazole was obtained from Synwit Technology. The solvents (pyridine, DMF and toluene) were dried by standard procedure and distilled before use.

Measurements and Instrumentation. ^{1}H NMR and ^{13}C NMR spectra were measured on a Bruker DMX-400 or Bruker DMX-600 spectrometer with *d*-chloroform as the solvent and tetramethylsilane as the internal reference. UV−visible absorption spectra were measured on a Hitachi U-3010 UV−vis spectrophotometer. Photoluminescence spectra were measured using a Hitachi F-4500 spectrophotometer. Melting points were determined on a WRS-1B Digital Melting Point Apparatus and were uncorrected. Mass spectra were recorded on a Shimadzu spectrometer. Elemental analyses were carried out on a flash EA 1112 elemental analyzer. Thermogravimetric analysis (TGA) was conducted on a Perkin-Elmer TGA-7 thermogravimetric analyzer at a heating rate of 20 °C/min and under a nitrogen flow rate of 100 mL/min. Gel permeation chromatography (GPC) measurements were conducted, using polystyrene as standard and THF as the eluent. The electrochemical cyclic voltammetry was conducted on a Zahner IM6e Electrochemical Workstation, in a 0.1 mol/L acetonitrile solution of tetrabutylammonium hexafluorophosphate (n-Bu_4NPF_6) at a potential scan rate of 100 mV/s with an Ag/Ag^+ reference electrode and a platinum wire counter electrode. Polymer film was formed by drop-casting 1.0 μL of polymer solutions in THF (analytical reagent, 1 mg/mL) onto the working electrode, and then dried in the air.

Device Fabrication and Characterization of PSCs. The PSCs were fabricated with a configuration of ITO/PEDOT:PSS (40 nm)/ active layer (40−90 nm)/Al (40 nm). A thin layer of PEDOT:PSS (poly(3,4-ethylenedioxythiophene): poly(styrenesulfonate)) was spin-cast on precleaned ITO-coated glass from a PEDOT:PSS aqueous solution (Baytron AI 4083 from H. C. Starck) at 2000 rpm and dried subsequently at 150 °C for 30 min in air, then the device was transferred to a glovebox, where the active layer of the blend of the copolymers and $PC_{70}BM$ was spin-coated onto the PEDOT:PSS layer. Finally, an Al top electrode was deposited in vacuum onto the active layer at a pressure of ca. 5×10^{-5} Pa. The active area of the device was defined by the mask when depositing Al and it was ca. 4 mm^2.

The thickness of the active layer was determined by an Ambios Tech. XP-2 profilometer. The current−voltage ($I-V$) characteristics were measured on a computer-controlled Keithley 236 Source-Measure Unit. A xenon lamp coupled with AM 1.5 solar spectrum filter was used as the light source, and the optical power at the sample was around 100 mW/cm^2.

Synthesis of the Monomers and Copolymers. The synthesis routes of the monomers and the copolymers are shown in Schemes 1 and 2. The detailed synthetic processes are as follows.

***N*-9′-Heptadecanyl-2,7-dibromocarbazole (2).** 2,7-Dibromocarbazole (15 g, 46.2 mmol), 9-heptadecane *p*-toluenesulfonate (20.8 g, 50.8 mmol) and the phase-transfer catalyst tetrabutylammonium hydrogensulfate(TBAHS, 0.3 g) were dissolved in 300 mL of acetone, followed by addition of 10.3 g (184 mmol) of powdered potassium hydroxide. The reaction mixture was stirred and refluxed for 2 h. After cooling to room temperature, the inorganic solids were filtered off and washed with acetone. After the combined filtrates were evaporated to dryness, water and hexane were added to the residue, and the organic layer was separated, washed with water twice, and dried over $MgSO_4$. After the organic solution was concentrated, the product was recrystallized from petroleum ether (60−90 °C) as a white solid at −20 °C, to get compound **2** in a yield of 85%. MS: m/z = 563 (M^+). Melting point: 67−68 °C. ^{1}H NMR (400 MHz, $CDCl_3$, δ, ppm): 7.90 (br, 2H); 7.70 (br, 1H); 7.54 (br, 1H); 7.33 (br, 2H) 4.42 (br, 1H); 2.19 (br, 2H); 1.90(br, 2H); 1.14 (br, 22H); 0.97 (br, 2H); 0.83 (t, J = 6.3 Hz, 6H). ^{13}C NMR (100 MHz, $CDCl_3$, δ, ppm): 143.11; 139.65; 122.54; 121.66; 121.41; 121.06; 119.99; 119.40; 114.73; 112.37; 57.16; 33.69; 31.94; 29.48; 29.33; 26.94; 22.81; 14.28. Anal. Calcd for $C_{29}H_{41}Br_2N$: C, 61.82; H, 7.33; N, 2.49; Br, 28.36. Found: C, 62.73; H, 7.50; N, 2.60; Br, 28.11.

2,7-Bis(4′,4′,5′,5′-tetramethyl-1′,3′,2′-dioxaborolan-2′-yl)-*N*-9″-heptadecanylcarbazole (3). A mixture of compound **2** (13.5 g, 24 mmol), bis(pinacolato)diboron (14.6 g, 57.6 mmol), (diphenylphosphino)ferrocene palladium dichloride ($PdCl_2$(dppf), 1.2 g,

Scheme 2. Synthesis Routes of PCzTPA−TVCN, PCzTPA−TVDCN, and PCzTPA−TVDT

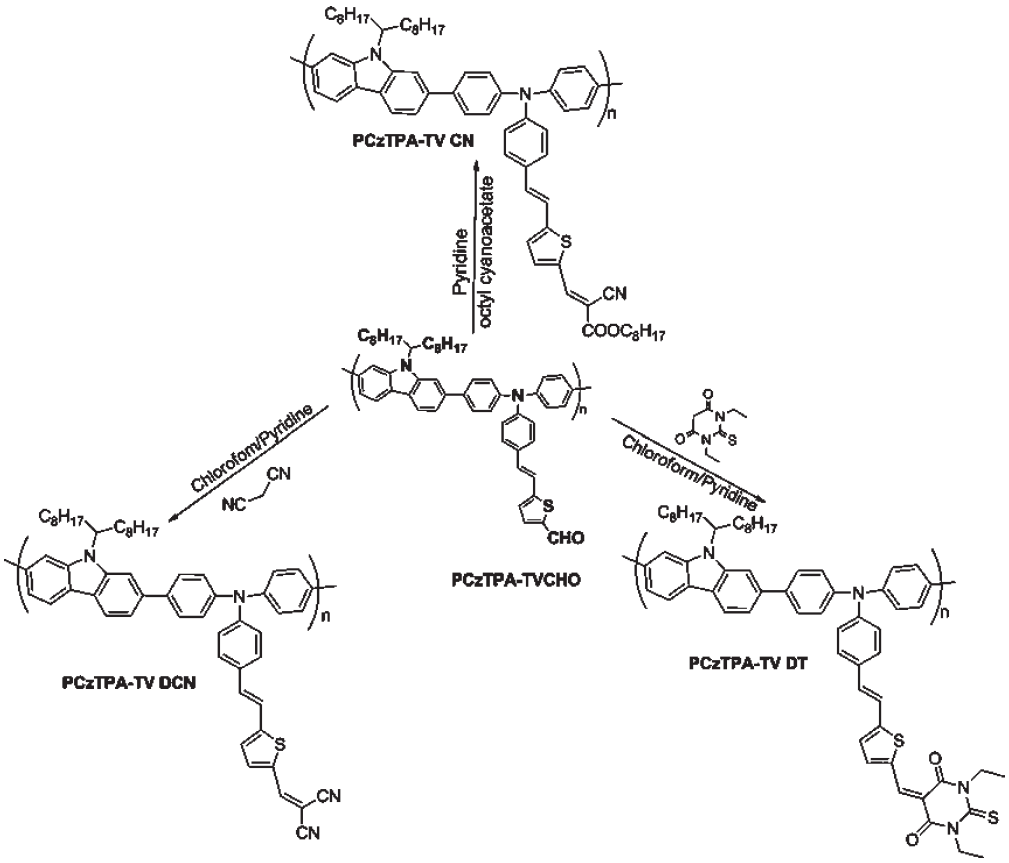

3.36 mmol), KOAc (16.5 g, 168 mmol), and degassed 1,4-dioxane (260 mL) was stirred under an argon atmosphere at 90 °C for 8 h. After cooling to room temperature, the crude mixture was filtered and washed with dichloromethane, and the filtrates were combined. Upon the removal of solvent, the dark-black residue was subjected to column chromatography on silica gel with ethyl acetate/hexane (v/v, 1:3) as the eluent, followed by recrystallization from ethanol to offer a white solid of **3** in a yield of 87%. MS: $m/z = 657$ (M^+). Melting point: 141−143 °C. ^{1}H NMR (400 MHz, $CDCl_3$, δ, ppm): 8.13 (t, J = 8.4 Hz, 2H,); 8.02 (S, 1H); 7.89 (S, 1H); 7.66 (d, J = 5.4 Hz, 2H); 4.70(t, J = 5 Hz, 2H); 2.33 (m, 2H); 1.90 (m, 2H); 1.61 (m, 2H); 1.39 (S, 24H); 1.19 (br, 24 H); 0.98(br, 2H); 0.87 (t, J = 6.4 Hz, 6H). ^{13}C NMR (100 MHz, $CDCl_3$, δ, ppm): 142.04; 138.78; 126.44, 126.41; 126.31; 126.28; 126.16; 124.78; 124.69; 120.13; 119.82; 118.19; 115.53; 83.76; 56.44; 33.92; 31.86; 29.41; 29.30; 26.85; 25.03; 22.70; 22.59; 14.17. Anal. Calcd for $C_{41}H_{65}B_2NO_4$: C, 74.89; H, 9.96; N, 2.13. Found: C, 74.70; H, 10.13; N, 2.20.

Synthesis of PCzTPA−TVCHO. 2,7-Bis(4,4,5,5-tetramethyl-1,3,2-dioxaborolane-2-yl)-*N*-9′-heptadecanylcarbazole (0.657 g, 1 mmol), compound **4** (4.311 g, 1 mmol), Aliquat 336 (20 mg) and $(PPh_3)_4Pd$ (34 mg, 0.03 mmol) (1.5 mol % based on total monomers) were dissolved in degassed toluene (6 mL) in a 25 mL two-necked round-bottom flask. A 2 M aqueous solution of K_2CO_3 (4 mL) was added. The solution was stirred vigorously under argon at 90 °C for 48 h. The resulting mixture was then poured into 250 mL of methanol. The precipitate was collected by filtration and washed with 2 M HCl and methanol. The yellowish-red solid product of **PCzTPA−TVCHO** was extracted with acetone for 24 h in a Soxhlet apparatus to remove oligomers and catalyst residues to yield **PCzTPA−TVCHO** as a yellowish-red solid (620 mg, yield: 79%). ^{1}H NMR (400 MHz, $CDCl_3$, δ, ppm): 9.85 (s, 1H), 8.20 (br, 2H),7.80 (s, 1H), 7.67(s, 5H), 7.60 (s, 1H), 7.48 (br, 5H), 7.32 (d, 8 Hz, 4H), 7.22 (d, 8 Hz, 4H), 7.14 (s, 2H), 4.68 (br, 1H), 2.34 (m, 2H), 1.98 (br, 2H), 1.26 (br, 8H), 1.12 (br,16H), 0.80 (t, J = 6.4 Hz, 6H). ^{13}C NMR (150 MHz, $CDCl_3$, δ, ppm): 182.50; 153.13; 148.30; 146.20; 143.16; 141.13; 139.84; 137.60; 137.41; 132.60; 132.18; 131.93; 129.93; 128.82; 128.58; 128.51; 128.08; 126.05; 125.12; 123.24; 120.69; 120.43; 119.03; 118.30; 109.68; 106.98; 56.484; 33.87; 31.80; 32.51; 29.51; 29.44; 29.39; 29.23; 26.94; 22.67; 22.63; 21.99; 14.10. Anal. Calcd for $C_{54}H_{58}N_2S$: C, 82.82; H, 7.47; N, 3.58; S, 4.09. Found: C, 82.70; H, 7.50; N, 3.49; S, 4.09.

Synthesis of PCzTPA−TVCN. A 20 equiv sample of octyl cyanoacetate (847 mg) was added to a solution of **PCzTPA−TVCHO** (168 mg, 0.25 mmol of basic units) in 20 mL of pyridine. The solution turned red immediately and was heated to 55 °C for 48 h. The solution was concentrated under reduced pressure, and the residue was added dropwise to excess methanol to precipitate the polymer of **PCzTPA−TVCN** as a red solid (120 mg). Further purification was performed by dissolution of the polymer in $CHCl_3$ (100 mL) and subsequently passing through a column packed with cotton and silica gel. The combined polymer solution was concentrated and was poured into methanol. ^{1}H NMR (400 MHz, $CDCl_3$, δ, ppm): 8.26 (s, 1H), 8.18 (br, 2H),7.76 (s, 1H), 7.68 (s, 4H), 7.63 (br, 1H), 7.48 (br, 5H), 7.22 (br, 4H), 7.17 (d, J = 8 Hz, 2H), 7.12 (s, 1H), 4.68 (br, 1H), 4.29 (dd, J = 6.4 Hz, 2H), 2.39 (br, 2H), 1.98 (br, 2H), 1.76 (br, 2H), 1.40 (br, 10 H), 1.12 (br, 24 H), 0.89 (t, J = 7.0 Hz, 3H), 0.80 (t, J = 6.4 Hz, 6H). ^{13}C NMR (150 MHz, CDCl3, δ, ppm): 163.22; 153.85; 148.47; 146.33; 146.132; 143.16; 139.84; 139.41; 137.68; 133.97; 133.27; 132.18; 132.11; 128.82; 128.54; 128.19; 127.66; 126.43; 125.25; 123.02; 120.69; 120.42; 118.66; 118.28; 116.33; 109.69; 106.99; 97.17; 66.57; 33.87; 31.80; 29.75; 29.52; 29.39; 29.23; 29.20; 28.626; 26.95; 25.86; 22.69; 22.63; 14.15; 14.11. Anal. Calcd for $C_{65}H_{75}N_3O_2S$: C, 81.12; H, 7.86; N, 4.37, S, 3.33. Found: C, 81.05; H, 7.90; N, 4.40; 3.35.

Synthesis of PCzTPA−TVDCN. A 20 equiv sample of malononitrile (282 mg) was added to a solution of **PCzTPA−TVCHO** (168 mg, 0.25 mmol of basic units) in a mixture of 20 mL of

chloroform and 1 mL pyridine. The solution turned purple immediately and was heated to 40 °C for 24 h. The solution was concentrated under reduced pressure, and the residue was added dropwise, to excess methanol to precipitate the polymer of **PCzTPA−TVDCN** as a purple solid (116 mg). Further purification of the polymer was carried out as that of **PCzTPA−TVCN**. ^{1}H NMR (400 MHz, $CDCl_3$, δ, ppm): 8.18 (m, 2H),7.80 (s, 1H), 7.74 (s, 1H), 7.68 (br, 4H), 7.60 (br, 1H), 7.47 (m, 4H), 7.32 (m, 4H), 7.22 (m, 4H), 7.14 (m, 2H), 4.68 (br, 1H), 2.34 (m, 2H), 1.98 (br, 2H), 1.26 (br, 8H), 1.12 (br, 16H), 0.80 (t, J = 6.4 Hz, 6H). ^{13}C NMR (150 MHz, CDCl3, δ, ppm): 155.82; 150.07; 148.89; 145.98; 143.14; 140.33; 139.83; 137.86; 134.65; 133.21; 132.10; 129.24; 128.82; 128.58; 128.51; 128.43; 126.50; 125.41; 122.67; 120.71; 120.44; 118.26; 118.04; 113.79; 109.70; 106.99; 56.48; 33.86; 31.79; 29.74; 29.50; 29.38; 29.22; 26.94; 22.62; 14.10. Anal. Calcd for $C_{57}H_{58}N_4S$: C, 82.37; H, 7.03; N, 6.74, S, 3.86. Found: C, 82.35; H, 7.13; N, 6.59; 3.92.

Synthesis of PCzTPA−TVDT. A 20 equiv sample of 1,3-diethyl-2-thiobarbituric acid (855 mg) was added to a solution of **PCzTPA−TVCHO** (168 mg, 0.25 mmol of basic units) in a mixture of 20 mL of chloroform and 1 mL pyridine. The solution turned blue immediately and was heated to 40 °C for 24 h. The solution was concentrated under reduced pressure, and the residue was added dropwise to excess methanol to precipitate the polymer of **PCzTPA−TVDT** as a dark blue solid (127 mg). Further purification of the polymer was carried out as that of **PCzTPA−TVCN**. ^{1}H NMR (400 MHz, $CDCl_3$, δ, ppm): 8.63 (s, 1H), 8.16 (br, 2H), 7.70 (m, 5H), 7.64 (s, 1H), 7.50 (r, 6H), 7.35 (m, 3H), 7.20(m, 3H), 4.68 (br, 5H), 2.39 (br, 2H), 1.98 (br, 2H), 1.26 (br, 30H), 0.80 (t, J = 6.4 Hz, 6H). ^{13}C NMR (150 MHz, CDCl3, δ, ppm): 178.68; 161.17; 160.95; 160.01; 149.12; 148.82; 147.54; 145.99; 143.15; 139.84; 137.86; 135.99; 134.73; 129.62; 128.82; 128.58; 128.48; 126.84; 125.42; 122.92; 122.73; 120.70; 120.45; 118.93; 118.27; 109.69; 109.41; 106.99; 56.49; 43.99; 43.18; 33.87; 31.80; 29.74; 29.51; 29.39; 29.23; 26.94; 22.63; 14.11; 12.60; 12.44. Anal. Calcd for $C_{62}H_{68}N_4O_2S_2$: C, 77.14; H, 7.10; N, 5.58, S, 6.64. Found: C, 77.20; H, 7.09; N, 5.49; 6.73.

Results and Discussion

Polymer Synthesis and Characterization. Chemical structures and synthetic routes of the main chain donor-side chain acceptor D−A copolymers are depicted in Schemes 1 and 2. The synthesis of alkylated compound **2** was well described by Leclerc et al. in a DMSO−KOH system.[29] To overcome the inconvenience brought by the high boiling point solvent (DMSO) along with low solubility of sulfonate in DMSO, we developed an easier synthesis procedure for Compound **2** in this work. The N-alkylation of 2,7-dibromocarbazole (**1**) was attained by the reaction with 9-heptadecane *p*-toluenesulfonate for 2 h using KOH as the base and acetone as the solvent, in the presence of TBAHS as a phase transfer reagent. The aryl bromide obtained was converted to the boronic ester using bis(pinacolato)diboron via Pd-mediated borylation. This procedure does not require generation of the corresponding lithiated species (which are very sensitive to air and moisture) typically used to form arylboronates.[33]

The dibromide, 2-[2-[4-[*N*,*N*-di(4-bromophenyl) amino]-phenyl]ethenyl]thien-5-al (**4**), was synthesized from commercially available triphenylamine in four steps.[26,32] The "basic" copolymer, viz. **PCzTPA−TVCHO**, was synthesized by Suzuki polycondensation of an equimolecular mixture of the diboronate (**3**) and dibromide (**4**), as illustrated in Scheme 1. The copolymerization was carried out for 48 h using $Pd(PPh_3)_4$ as the catalyst in a two-phase mixture of degassed toluene and aqueous K_2CO_3 (2.0 M) and in the presence of Aliquat 336 as the phase transfer reagent. To study the structure−property relationship, polymers with similar molecular architecture and bearing comparable numbers of conjugation units are desirable.[34] To overcome the reactivity difference among the monomers, a postmodification approach was adopted to modify the pendant groups on the thienylenevinylene side chains of **PCzTPA−TVCHO**, forming **PCzTPA−TVCN**, **PCzTPA−TVDCN**, and **PCzTPA−TVDT**. Thus, all the three polymers have the same number of conjugation units as **PCzTPA−TVCHO** with fine-tuned electronic structure.

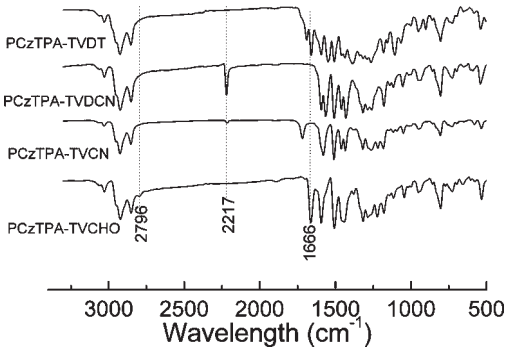

Figure 1. FT-IR spectra of the copolymers.

For the synthesis of **PCzTPA−TVCN**, the optimum reaction condition to achieve complete conversion of the aldehyde groups was found to be at 55 °C for 48 h in pyridine as both solvent and base, while for **PCzTPA−TVDCN** and **PCzTPA−TVDT**, the optimum reaction condition is in chloroform at 40 °C for 24 h and using 1 mL pyridine as base. After purification and drying, **PCzTPA−TVCHO**, **PCzTPA−TVCN**, **PCzTPA−TVDCN**, and **PCzTPA−TVDT** were obtained as yellowish-red, red, purple, and dark blue solids, respectively, indicating significant change in their optical properties. The bulky alkyl side chains attaching on the nitrogen atom of the carbazole unit combined with the amorphous nature of the triphenylamine group, account for the high solubility of the copolymers in chlorinated solvents, such as dichloromathane, chloroform and dichlorobenzene, which is important for their application in PSCs.

The conversion of aromatic aldehyde of **PCzTPA−TVCHO** to other acceptor groups was confirmed by Fourier transform infrared (FT-IR) absorption spectroscopy. As shown in Figure 1, the characteristic absorption peaks of the −CHO group appeared at 1666 and 2796 cm^{-1}, belonging to the C−H and C═O stretching vibrations, respectively.[35] After transformation into **PCzTPA−TVCN** and **PCzTPA−TVDCN**, these characteristic absorptions of aldehyde disappeared, and new absorption peaks at 2217 cm^{-1} (corresponding to C≡N stretching for the two polymers) and 1710 cm^{-1} (corresponding to C═O stretching for **PCzTPA−TVCN**) emerged, indicative of complete conversion of the terminal aldehyde group. It should be noted that for **PCzTPA−TVDT**, due to overlapping of vibration in the aldehyde group and that of 1,3-diethyl-2-thiobarbituric acid moiety, the conversion of aldehyde group into the 1,3-diethyl-2-thiobarbituric acid group in **PCzTPA−TVDT** cannot be identified in the FT-IR spectrum. However, it can be clearly confirmed in the ^{1}H NMR spectra. In the ^{1}H NMR spectra (see Figure S1 in the Supporting Information), the complete disappearance of the aldehyde proton signal at 9.8 ppm[10] and the appearance of olefinic proton signals at 8.26 ppm for **PCzTPA−TVCN**, 7.74 ppm for **PCzTPA−TVDCN**, and 8.62 ppm[27] for **PCzTPA−TVDT**, confirmed the complete structural conversion. In addition, the ratios of integrated peak areas of olefinic to aliphatic protons and that of olefinic to methine group adjacent to the carbazole *N* atom protons are consistent with the proposed structures of

Table 1. Molecular Weights, Thermal Properties, and Physical Properties of the Copolymers

polymers	M_n (g/mol)	PDI (M_w/M_n)	T_d[a] (°C)	λ_{abs}[b] (nm)	E_g[c] (eV)	HOMO[d] (eV)	LUMO[e] (eV)
PCzTPA−TVCHO	14.2K	3.93	360	269, 388, 445	2.38	−5.27	−2.89
PCzTPA−TVCN	18.7K	3.58	289	270, 385, 519	2.00	−5.29	−3.29
PCzTPA−TVDCN	15.9K	3.62	399	271, 383, 548	1.89	−5.30	−3.41
PCzTPA−TVDT	19.8K	3.49	264	269, 380, 588	1.74	−5.29	−3.55

[a] 5% weight loss temperature measured by TGA under N_2. [b] For the polymer films. [c] Band gap, estimated from the optical absorption band edge of the films. [d] Calculated from the onset oxidation potentials of the polymers. [e] Estimated using empirical equations $E_{LUMO} = E_{HOMO} + E_g$.

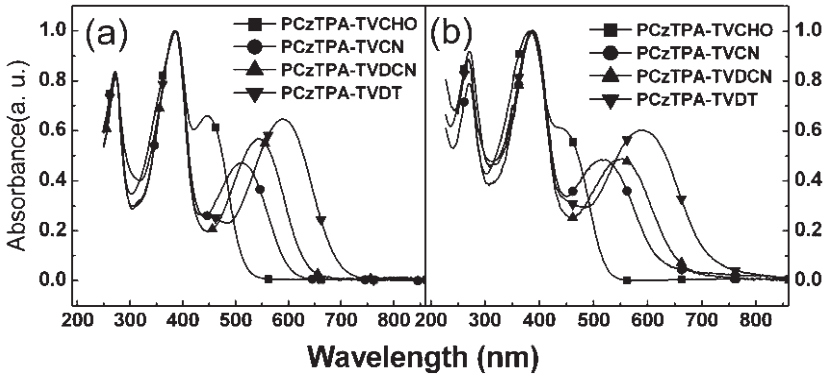

Figure 2. UV−visible absorption spectra of the copolymers (a) in toluene solutions and (b) in films.

PCzTPA−TVCN, **PCzTPA−TVDCN**, and **PCzTPA−TVDT**, as depicted in Scheme 2.

Molecular weight of the polymers was determined by gel permeation chromatography (GPC). Number-average molecular weight (M_n) of **PCzTPA−TVCHO** is 1.42×10^4 g/mol, corresponding to a polymerization degree of ca. 18, with a polydispersity index of 3.93. The structural transformation of **PCzTPA−TVCHO** into other three copolymers has led to a slight increase in molecular weights of the resulting copolymers, as shown in Table 1. The M_n's of **PCzTPA−TVCN**, **PCzTPA−TVDCN**, and **PCzTPA−TVDCN** were found to be 1.87×10^4, 1.59×10^4, and 1.98×10^4 g/mol respectively, with the corresponding polydispersity indices of 3.58, 3.62, and 3.49.

Thermal Stability. Thermal property of the copolymers was determined via thermogravimetric analysis (TGA) under a nitrogen atmosphere. As shown in Table 1 and Figure S2 (see Supporting Information), the 5% weight-loss temperatures for **PCzTPA−TVCN**, **PCzTPA−TVDCN**, and **PCzTPA−TVDT** are in the range of 264−399 °C, which is adequate for application of the copolymers as active materials in the optoelectronic devices.[36]

Optical Properties. Figure 2 shows the absorption spectra of the copolymers in solutions and in solid films. All the polymers are featured by three distinct absorption peaks. In the polymer solutions, the sharp absorption peak around 270 nm originates from n−π^* transition of the backbone,[37] the maximum absorptions of the copolymers at 388 nm for **PCzTPA−TVCHO**, 385 nm for **PCzTPA−TVCN,** 383 nm for **PCzTPA−TVDCN**, and 380 nm for **PCzTPA−TVDT** (Figure 2a), correspond to the $\pi-\pi^*$ transition of the polymer backbone. The $\pi-\pi^*$ transition absorption peaks of the polymer backbones, are slightly blue-shifted when the pendant acceptor groups are varied from the aldehyde group to the monocyano group, to the dicyano group and further to 1,3-diethyl-2-thiobarbituric acid group. This phenomenon is probably related to the increasing extent of distortion of the backbones, thereby reducing the effective conjugation length of the TPA-containing copolymers.[10]

In addition to the absorptions of carbazole-*alt*-TPA backbones, the introduction of electron-withdrawing pendant groups produces new absorption bands at 445 nm for **PCzTPA−TVCHO**, 519 nm for **PCzTPA−TVCN**, 548 nm for **PCzTPA−TVDCN**, and 588 nm for **PCzTPA−TVDT**, attributable to the intramolecular charge transfer (ICT) interaction[10,38] between the polymer backbone and the pendant acceptor groups. Thus, both the main chain and side chain contribute to the broad nature of the absorption spectra of the copolymers, which is much like that of the conjugated side chain polymers developed in our group.[18] Evidently, the ICT interactions are progressively enhanced with the increase of the electron affinity of the pendant acceptor group in the D−A copolymers, due to the enhanced electron accepting ability of the acceptor moiety.[10] For the as-spun film on quartz substrate, the UV−visible absorption spectra of the copolymers are red-shifted and broadened (Figure 2b), as compared with that of their corresponding dilute solutions. The red-shift and broadening of the absorption spectra of the polymer films is a common phenomenon, which results from the enhanced interchain interaction in the solid films and is probably related to increased polarizability of the film.[10] It seems that the interchain interaction in the main chain donor-side chain acceptor D−A copolymers is not as strong as those of the main chain D−A copolymers, probably due to the fact that the bulky side chains and propeller-twisting conformation of the TPA moiety retard the conformation change of the polymer chains in the solid state.[38,39] The absorption edges of the copolymer films are located at 521 nm, 620 nm, 656 and 713 nm for **PCzTPA−TVCHO**, **PCzTPA−TVCN**, **PCzTPA−TVDCN**, and **PCzTPA−TVDT** respectively, from which the optical bandgaps were calculated to be 2.38 eV for **PCzTPA−TVCHO**, 2.00 eV for **PCzTPA−TVCN**, 1.89 eV for **PCzTPA−TVDCN**, and 1.74 eV for **PCzTPA−TVDT**. The absorption peak wavelength and optical bandgaps of the copolymer films are also listed in Table 1. The variation in the absorption and bandgap suggests the possibility of tuning the photophysical properties by the simple manipulation of acceptor strength in the pendant groups.

Electrochemical Properties and Electronic Energy Levels. The highest occupied molecular orbital (HOMO) and lowest unoccupied molecular orbital (LUMO) energy levels of the

conjugated polymers are important parameters in the design of optoelectronic devices, and they can be estimated from the onset oxidation and reduction potentials.[40] Figure S3 (see Supporting Information) shows the cyclic voltammograms of the four copolymers. The onset oxidation potentials (E_{ox}^{onset}) are 0.56 V for **PCzTPA−TVCHO**, 0.58 V for **PCzTPA−TVCN**, 0.59 V for **PCzTPA−TVDCN**, and 0.58 V vs. Ag/Ag^+ for **PCzTPA−TVDT**. The HOMO energy levels of the polymers were estimated according to the following equations:[41] $E_{HOMO} = -e(E_{ox}^{onset}+4.71)$ (eV), where the unit of E_{ox}^{onset} is V vs. Ag/Ag^+. The HOMO levels of **PCzTPA−TVCHO**, **PCzTPA−TVCN**, and **PCzTPA−TVDCN**, calculated in this way, are −5.27, −5.29, and −5.30, and −5.29 eV, respectively, as listed in Table 1. Since we could not obtain reliable onset reduction potentials for the four copolymers, the optical band gaps (E_g) of the polymer films (which were calculated from their absorption band edge) were utilized to estimate the LUMO energy levels of the copolymers based on the relation of $E_g = E_{LUMO} - E_{HOMO}$. The estimated LUMO energy levels of **PCzTPA−TVCHO**, **PCzTPA−TVCN** and **PCzTPA−TVDCN**, and **PCzTPA−TVDT** are −2.89, −3.29, −3.41, and −3.55 eV, respectively, which are also shown in Table 1. Obviously, the HOMO energy levels of the four copolymers remain almost unchanged, in spite of the presence of different pendant acceptor groups, while their LUMO energy levels decreased after attaching the acceptor cyano and 1,3-diethyl-2-thiobarbituric acid (DT) acceptor groups in the conjugated side chains on the TPA units. Regarding that the threshold HOMO level for air stable conjugated polymers being estimated to be −5.2 eV,[42,43] lower HOMO levels of the three copolymers with cyano and DT acceptor groups should be beneficial to their chemical stability in ambient conditions. In addition, the deeper HOMO level of the copolymers is desirable for higher open circuit voltage (V_{oc}) of the PSCs with polymers as donor materials because the V_{oc} is usually proportional to the difference between the LUMO level of the acceptor and the HOMO level of the donor.[9]

Theoretical Calculations. To provide further insight into the fundamentals of molecular architecture, molecular simulation was carried out for **PCzTPA−TVCHO**, **PCzTPA−TVCN**, **PCzTPA−TVDCN**, and **PCzTPA−TVDT** with a chain length of $n = 1$ at the DFT B3LYP/6-31G(d) level with the Gaussian 03 program package.[44] The bulky *N*-alkyl chain was not included in the calculation to avoid excessive computation demand, since they do not significantly affect the equilibrium geometry and thus the electronic properties. All C=C bonds outside the aromatic rings were set to be in trans configuration. As depicted in Figure 3, the LUMOs for all the four polymers are located on the peripheral triphenylamine groups and the adjacent carbazole rings, and the computed HOMO values are close to one another for the four polymers. The electron density distributions at LUMO become highly localized near the electron-withdrawing group, and the well-separated distribution of HOMO and LUMO levels indicate that a transition between them can be considered as a charge-transfer transition. The unique electron distribution patterns of **PCzTPA−TVCN, PCzTPA−TVDCN**, and **PCzTPA−TVDT** have the advantage of allowing charge separation through sequential transfer of electrons from the main chains to the side chain acceptor groups and then to fullerene acceptor in a bulk-heterojunction PSC. Also, it can be envisioned from the DFT results that LUMO energy levels can be further decreased by appending a stronger pedant acceptor within this molecular architecture, indicative of flexibility of this special main chain donor-side chain acceptor D−A copolymer architecture for tuning the optoelectronic properties of the conjugated polymers.

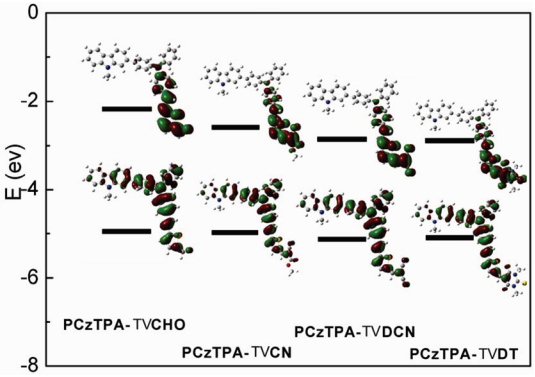

Figure 3. HOMO and LUMO energy levels and the frontier molecular orbital obtained from DFT calculations on **PCzTPA−TVCHO**, **PCzTPA−TVCN**, **PCzTPA−TVDCN**, and **PCzTPA−TVDT** with a chain length $n = 1$ at the B3LYP/6-31G* level of theory.

Table 2. Photovoltaic Parameters of the PSCs Based on Copolymer/$PC_{70}BM$ (1:4, w/w)

copolymers	V_{oc} (V)	J_{sc} (mA cm^{-2})	FF (%)	PCE (%)	thickness (nm)
PCzTPA−TVCN	0.79	6.41	0.383	1.94	60
PCzTPA−TVDCN	0.84	7.00	0.415	2.44	67
PCzTPA−TVDT	0.87	7.50	0.424	2.76	60

In addition, it can be seen from Figure 3 and Table 1 that although discrepancies exist between the calculation and experimental results, the trends of variation in the HOMO and LUMO energy levels, as well as the energy gaps, are similar. The presence of pendant cyano and 1,3-diethyl-2-thiobarbituric acid groups with strong electron affinity leads to the decrease of the LUMO energy levels of **PCzTPA−TVCN**, **PCzTPA−TVDCN**, and **PCzTPA−TVDT** but affects their HOMO levels to a much lesser extent. This phenomenon is significantly different from most main chain D−A type copolymers, whose HOMO levels were elevated a lot when using different acceptors to reduce the band gaps.[45]

Photovoltaic Properties. Bulk heterojunction PSCs using the three copolymers **PCzTPA−TVCN**, **PCzTPA−TVDCN**, and **PCzTPA−TVDT** as donor and $PC_{70}BM$ as acceptor were investigated with the device configuration of ITO/PEDOT:PSS/copolymer:$PC_{70}BM$(1:4, w/w)/Al. Photovoltaic performance characteristics of the PSCs are summarized in Table 2. $PC_{70}BM$ was chosen as the acceptor because it has stronger absorption in the visible region from 400 to 530 nm,[46] which can complement the absorption valley between the $\pi-\pi$ transition of the backbone and ICT interactions, as demonstrated by the absorption spectra of the polymer film (Figure 2) and the polymer/$PC_{70}BM$ blend film (see Figure S4 in Supporting Information). Figure 4 shows the current density−voltage ($J-V$) curves of the PSCs based on the copolymers/$PC_{70}BM$. **PCzTPA−TVDT** demonstrated better photovoltaic performance over the other two copolymers with J_{sc} of 7.5 mA/cm^2, FF of 0.42, V_{oc} of 0.87 V, corresponding to a PCE of 2.76%. For PSCs based on the three copolymers as donor, the V_{oc} is around ~0.8 V, which is similar to that of the PSCs based on other carbazole copolymer donors. The high V_{oc} is the result of the lower HOMO level of the copolymers. From **PCzTPA−TVCN** to **PCzTPA−TVDCN** and further to **PCzTPA−TVDT**, the progressively improved absorption spectra brought by the enhanced ICT interaction, should account for the increase in J_{sc}. The incident-photon-to-converted current efficiency (IPCE) spectra of the PSCs, as shown

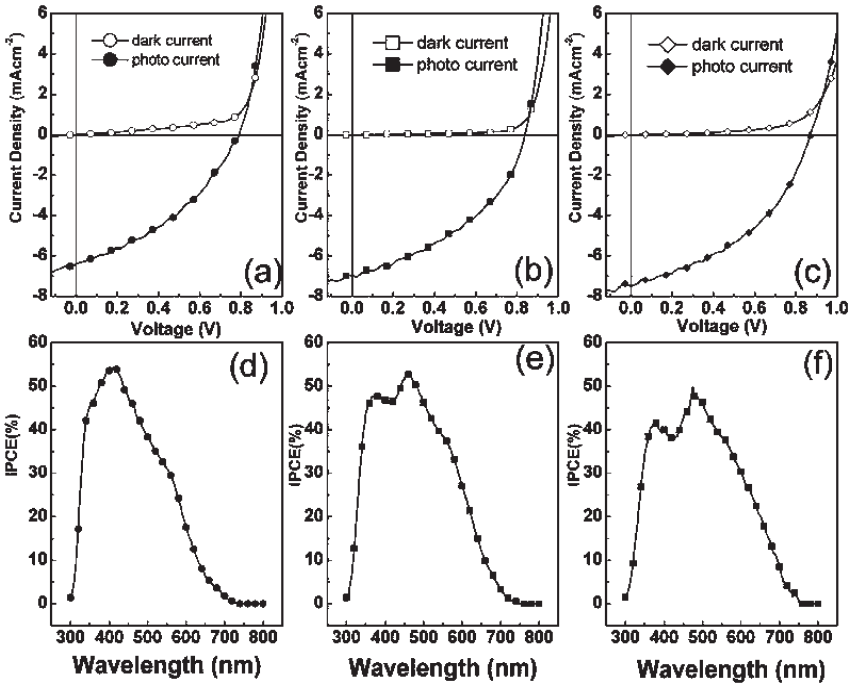

Figure 4. Current density−voltage characteristics of PSCs based on the 1:4 weight ratio composite films of **PCzZTPA−TVCN**:$PC_{70}BM$ (a), **PCzTPA−TVDCN**:$PC_{70}BM$ (b), and **PCzTPA−TVDT**:$PC_{70}BM$ (c). The incident-photon-to-converted-current efficiency (IPCE) spectra of the corresponding devices: **PCzTPA−TVCN**:$PC_{70}BM$ (d), **PCzTPA−TVDCN**:$PC_{70}BM$ (e), and **PCzTPA−TVDT**:$PC_{70}BM$ (f).

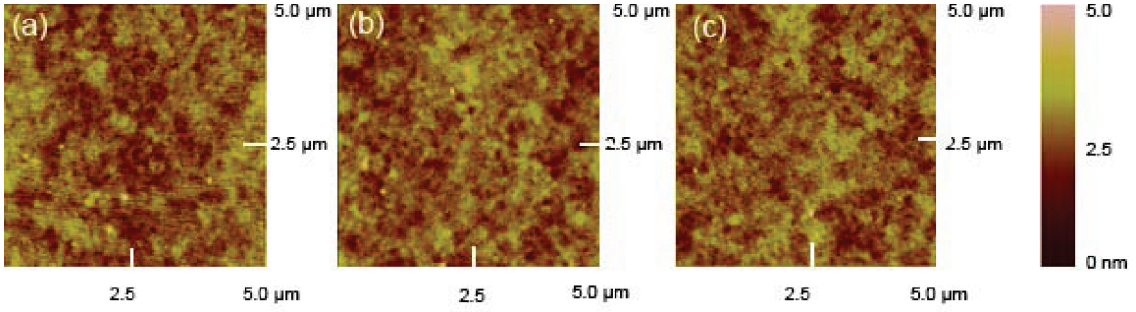

Figure 5. Tapping mode AFM topography images (5 × 5 μm^2) of the 1:4 (weight ratio) composite films of (a) **PCzTPA−TVCN**/$PC_{70}BM$, (b) **PCzTPA−TVDCN**/$PC_{70}BM$, and (c) **PCzTPA−TVDT**/$PC_{70}BM$.

in Figure 4, are consistent with the absorption spectra of the blend films of the active layer and the short circuit current values of the PSCs.

AFM Morphology. The morphologies of the blend films of $PC_{70}BM$ and the three copolymers **PCzTPA−TVCN**, **PCzTPA−TVDCN**, and **PCzTPA−TVDT** were investigated by atomic force microscopy (AFM). As shown in Figure 5, all the blend films show smooth surface with root-mean-square (rms) roughness of 0.50 nm for **PCzTPA−TVCN**, 0.45 nm for **PCzTPA−TVDCN**, and 0.47 nm for **PCzTPA−TVDT**, indicating excellent miscibility between the copolymers and $PC_{70}BM$. As suggested by the optimized geometry of the copolymers, the two-dimensional architecture combined with twisted propeller conformation of the TPA moiety would create large free volume, where fullerene molecules can be dispersed well over the polymer network, thus no evident phase separation was observed. Although the well-distribution of fullerene molecules over polymer network can offer large heterojunction interface area for exciton dissociation, proper phase separation is desirable in the composite films to enable a continuous percolating path for hole and electron transport to the corresponding electrodes. Therefore, it can be expected that even better device performance could be achieved, by further device engineering, such as thermal annealing, solvent annealing, and additives to promote proper phase separation.

Conclusions

A conjugated alternating copolymer of carbazole and triphenylamine bearing the thienylene-vinylene conjugated side chain with aldehyde terminal group, **PCzTPA−TVCHO**, was synthesized via the Suzuki coupling method. Then three copolymers, with the side chains containing acceptor groups of monocyano (**PCzTPA−TVCN**), dicyano (**PCzTPA−TVDCN**), and 1,3-diethyl-2-thiobarbituric acid (**PCzTPA−TVDT**), were synthesized via chemical transformation of the aldehyde group in **PCzTPA−TVCHO**, into respective acceptor groups. The synthesis strategy allows direct comparison of polymers with the same number of conjugation units for elucidating their structure−property relationships. The copolymers exhibit good solubility in common organic solvents and good thermal stability. Through manipulating the strength of the acceptor groups attached at the conjugated side chain of the copolymer backbone, the energy levels, and thus

the photophysical and electronic properties, as well as the absorption spectra of the copolymers were effectively tuned. The power conversion efficiency of the PSCs based on the copolymers/$PC_{70}BM$ (1:4, w/w) reached 1.94% for **PCzTPA−TVCN**, 2.44% for **PCzTPA−TVDCN** and 2.76% for **PCzTPA−TVDT**, under the illumination of AM1.5, 100 mW/cm^2. The chemical transformation approach thus provides a simple and effective way for tuning the optoelectronic properties of the conjugated polymers.

Acknowledgment. This work was supported by NSFC (Nos. 50633050, 20721061 and 50933003), and the Chinese Academy of Sciences. The authors thank Dr. Shanghui Ye for the AFM measurements.

Supporting Information Available: Figures showing ^{1}H NMR spectra, TGA plots and cyclic voltammograms of the polymers, and UV−vis absorption spectra of the blend films of copolymer/$PC_{70}BM$. This material is available free of charge via the Internet at http://pubs.acs.org.

References and Notes

(1) Yu, G.; Gao, J.; Hummelen, J. C.; Wudl, F.; Heeger, A. J. *Science* **1995**, *270*, 1789.
(2) Li, Y. F.; Zou, Y. P. *Adv. Mater.* **2008**, *20*, 2952.
(3) Chen, J.; Cao, Y. *Acc. Chem. Res.* **2009**, *42*, 1709.
(4) Liang, Y.; Wu, Y.; Feng, D.; Tsai, S.-T.; Son, H.-J.; Li, G.; Yu, L. *J. Am. Chem. Soc.* **2008**, *131*, 56.
(5) Kim, J. Y.; Lee, K.; Coates, N. E.; Moses, D.; Nguyen, T.-Q.; Dante, M.; Heeger, A. J. *Science* **2007**, *317*, 222.
(6) Inganäs, O.; Zhang, F.; Tvingstedt, K.; Andersson, L. M.; Hellström, S.; Andersson, M. R. *Adv. Mater.* **2010**, *22*, E100.
(7) Peet, J.; Kim, J. Y.; Coates, N. E.; Ma, W. L.; Moses, D.; Heeger, A. J.; Bazan, G. C. *Nat. Mater.* **2007**, *6*, 497.
(8) Liang, Y.; Feng, D.; Wu, Y.; Tsai, S.-T.; Li, G.; Ray, C.; Yu, L. *J. Am. Chem. Soc.* **2009**, *131*, 7792.
(9) Thompson, B. C.; Fréchet, J. M. J. *Angew. Chem., Int. Ed.* **2008**, *47*, 58.
(10) Zhang, Z.-G.; Zhang, K.-L.; Liu, G.; Zhu, C.-X.; Neoh, K.-G.; Kang, E.-T. *Macromolecules* **2009**, *42*, 3104.
(11) Wettach, H.; Pasker, F.; Hoger, S. *Macromolecules* **2008**, *41*, 9513.
(12) Zhang, Y.; Hau, S. K.; Yip, H.-L.; Sun, Y.; Acton, O.; Jen, A. K. Y. *Chem. Mater.* **2010**, *22*, 2696.
(13) Zheng, Q.; Jung, B. J.; Sun, J.; Katz, H. E. *J. Am. Chem. Soc.* **2010**, *132*, 5394.
(14) Wu, J.-S.; Cheng, Y.-J.; Dubosc, M.; Hsieh, C.-H.; Chang, C.-Y.; Hsu, C.-S. *Chem. Commun.* **2010**, *46*, 3259.
(15) Hou, J.; Chen, H.-Y.; Zhang, S.; Li, G.; Yang, Y. *J. Am. Chem. Soc.* **2008**, *130*, 16144.
(16) Huo, L.; Hou, J.; Zhang, S.; Chen, H.-Y.; Yang, Y. *Angew. Chem., Int. Ed.* **2010**, *49*, 1500.
(17) Price, S. C.; Stuart, A. C.; You, W. *Macromolecules* **2010**, *43*, 4609.
(18) Zhang, X.; Steckler, T. T.; Dasari, R. R.; Ohira, S.; Potscavage, W. J., Jr; Tiwari, S. P.; Coppee, S.; Ellinger, S.; Barlow, S.; Bredas, J.-L.; Kippelen, B.; Reynolds, J. R.; Marder, S. R. *J. Mater. Chem.* **2010**, *20*, 123.
(19) Zhou, E.; Cong, J.; Yamakawa, S.; Wei, Q.; Nakamura, M.; Tajima, K.; Yang, C.; Hashimoto, K. *Macromolecules* **2010**, *43*, 2873.
(20) Zou, Y.; Najari, A.; Berrouard, P.; Beaupré, S.; Réda Aïch, B.; Tao, Y.; Leclerc, M. *J. Am. Chem. Soc.* **2010**, *132*, 5330.
(21) Piliego, C.; Holcombe, T. W.; Douglas, J. D.; Woo, C. H.; Beaujuge, P. M.; Fréchet, J. M. J. *J. Am. Chem. Soc.* **2010**, *132*, 7595.
(22) Zhou, E.; Wei, Q.; Yamakawa, S.; Zhang, Y.; Tajima, K.; Yang, C.; Hashimoto, K. *Macromolecules* **2009**, *43*, 821.
(23) Hou, J.; Tan, Z. a.; Yan, Y.; He, Y.; Yang, C.; Li, Y. *J. Am. Chem. Soc.* **2006**, *128*, 4911.
(24) (a) Wang, Y.; Zhou, E.; Liu, Y. Q.; Xi, H.; Ye, S.; Wu, W.; Guo, Y.; Di, C.; Sun, Y.; Yu, G.; Li, Y. F. *Chem. Mater.* **2007**, *19*, 3361. (b) Zou, Y. P.; Wu, W. P.; Sang, G. Y.; Yang, Y.; Liu, Y. Q.; Li, Y. F. *Macromolecules* **2007**, *40*, 7231.
(25) Chang, Y. T.; Hsu, S. L.; Chen, G. Y.; Su, M. H.; Singh, T. A.; Diau, E. W. G.; Wei, K. H. *Adv. Funct. Mater.* **2008**, *18*, 2356.
(26) Huang, F.; Chen, K.-S.; Yip, H.-L.; Hau, S. K.; Acton, O.; Zhang, Y.; Luo, J.; Jen, A. K. Y. *J. Am. Chem. Soc.* **2009**, *131*, 13886.
(27) Duan, C.; Cai, W.; Huang, F.; Zhang, J.; Wang, M.; Yang, T.; Zhong, C.; Gong, X.; Cao, Y. *Macromolecules* **2010**, *43*, 5262.
(28) Blouin, N.; Leclerc, M. *Acc. Chem. Res.* **2008**, *41*, 1110.
(29) Blouin, N.; Michaud, A.; Leclerc, M. *Adv. Mater.* **2007**, *19*, 2295.
(30) Qin, R.; Li, W.; Li, C.; Du, C.; Veit, C.; Schleiermacher, H.-F.; Andersson, M.; Bo, Z.; Liu, Z.; Inganäs, O.; Wuerfel, U.; Zhang, F. *J. Am. Chem. Soc.* **2009**, *131*, 14612.
(31) Blouin, N.; Michaud, A.; Gendron, D.; Wakim, S.; Blair, E.; Neagu-Plesu, R.; Belletête, M.; Durocher, G.; Tao, Y.; Leclerc, M. *J. Am. Chem. Soc.* **2007**, *130*, 732.
(32) Zhang, W.; Fang, Z.; Su, M.; Saeys, M.; Liu, B. *Macromol. Rapid Commun.* **2009**, *30*, 1533.
(33) Kotha, S.; Lahiri, K.; Kashinath, D. *Tetrahedron* **2002**, *58*, 9633.
(34) Pokrop, R.; Verilhac, J. M.; Gasior, A.; Wielgus, I.; Zagorska, M.; Travers, J. P.; Pron, A. *J. Mater. Chem.* **2006**, *16*, 3099.
(35) Fang, Q.; Yamamoto, T. *Macromolecules* **2004**, *37*, 5894.
(36) Li, J. Y.; Liu, D.; Li, Y. Q.; Lee, C. S.; Kwong, H. L.; Lee, S. T. *Chem. Mater.* **2005**, *17*, 1208.
(37) Pu, Y.-J.; Soma, M.; Kido, J.; Nishide, H. *Chem. Mater.* **2001**, *13*, 3817.
(38) Leriche, P.; Frère, P.; Cravino, A.; Alévêque, O.; Roncali, J. *J. Org. Chem.* **2007**, *72*, 8332.
(39) Surin, M.; Sonar, P.; Grimsdale, A. C.; Mullen, K.; De Feyter, S.; Habuchi, S.; Sarzi, S.; Braeken, E.; Heyen, A. V.; Van der Auweraer, M.; De Schryver, F. C.; Cavallini, M.; Moulin, J. F.; Biscarini, F.; Femoni, C.; Roberto, L.; Leclere, P. *J. Mater. Chem.* **2007**, *17*, 728.
(40) Li, Y.; Cao, Y.; Gao, J.; Wang, D.; Yu, G.; Heeger, A. J. *Synth. Met.* **1999**, *99*, 243.
(41) Sun, Q.; Wang, H.; Yang, C.; Li, Y. *J. Mater. Chem.* **2003**, *13*, 800.
(42) Thompson, B. C.; Kim, Y.-G.; Reynolds, J. R. *Macromolecules* **2005**, *38*, 5359.
(43) de Leeuw, D. M.; Simenon, M. M. J.; Brown, A. R.; Einerhand, R. E. F. *Synth. Met.* **1997**, *87*, 53.
(44) Gaussian 03, R. E.; Frisch, M. J.; Trucks, G. W.; Schlegel, H. B.; Scuseria, G. E.; Robb, M. A.; Cheeseman, J. R.; Montgomery, J. A.; Vreven, J., T.; Kudin, K. N.; Burant, J. C.; Millam, J. M.; Iyengar, S. S.; Tomasi, J.; Barone, V.; Mennucci, B.; Cossi, M.; Scalmani, G.; Rega, N.; Petersson, G. A.; Nakatsuji, H.; Hada, M.; Ehara, M.; Toyota, K.; Fukuda, R.; Hasegawa, J.; Ishida, M.; Nakajima, T.; Honda, Y.; Kitao, O.; Nakai, H.; Klene, M.; Li, X.; Knox, J. E.; Hratchian, H. P.; Cross, J. B.; Bakken, V.; Adamo, C.; Jaramillo, J.; Gomperts, R.; Stratmann, R. E.; Yazyev, O.; Austin, A. J.; Cammi, R.; Pomelli, C.; Ochterski, J. W.; Ayala, P. Y.; Morokuma, K.; Voth, G. A.; Salvador, P.; Dannenberg, J. J.; G., Z. V.; Dapprich, S.; Daniels, A. D.; Strain, M. C.; Farkas, O.; Malick, D. K.; Rabuck, A. D.; Raghavachari, K.; Foresman, J. B.; Ortiz, J. V.; Cui, Q.; Baboul, A. G.; Clifford, S.; Cioslowski, J.; Stefanov, B. B.; Liu, G.; Liashenko, A.; Piskorz, P.; Komaromi, I.; Martin, R. L.; Fox, D. J.; Keith, T.; Al-Laham, M. A.; Peng, C. Y.; Nanayakkara, A.; Challacombe, M.; Gill, P. M. W.; Johnson, B.; Chen, W.; Wong, M. W.; Gonzalez, C.; Pople, J. A. Gaussian, Inc.: Wallingford CT, 2004.
(45) Hou, J.; Park, M.-H.; Zhang, S.; Yao, Y.; Chen, L.-M.; Li, J.-H.; Yang, Y. *Macromolecules* **2008**, *41*, 6012.
(46) Yao, Y.; Shi, C.; Li, G.; Shrotriya, V.; Pei, Q.; Yang, Y. *Appl. Phys. Lett.* **2006**, *89*, 153507.